"X-Ray and Backscattering Analysis of Ion Implantation Phenomena in GaAs and Related Compounds"

MID-TERM TECHNICAL REPORT

ARPA Order Number:	4550
Contractor:	California Institute of Technology
Effective Date of Contract:	August 5, 1982
Contract Expiration Date:	August 4, 1984
Reporting Period:	May 5, 1983 - August 4, 1983
Contract Number:	MDA 903-82-C-0348
Principal Investigators:	Professor M-A. Nicolet (213) 356-4803 Professor T. Vreeland, Jr. (213) 356-4431

"The views and conclusions contained in this document are those of the authors and should not be interpreted as representing the official policies, either expressed or implied, of the Defense Advanced Research Projects Agency or the U.S. Government."

Sponsored by

Defense Advanced Research Projects Agency (DoD)
ARPA Order No. 4550

Under Contract No. MDA 903-82-C-0348 issued by
Department of the Army, Defense Supply Service - Washington,
Washington, D. C. 20310

MID-TERM TECHNICAL REPORT

1. Introduction

It is well-known that amorphous GaAs layers produced by ion implantation behave differently upon thermal annealing from amorphized layers of Si or Ge[1]. The special features of GaAs include non-linear regrowth with time, poor epitaxy at low temperatures, and the necessity of high annealing temperatures for electrical activation. Whilst many models have been proposed, the reasons for these differences are unclear. Double crystal x-ray diffractrometry, interpreted with a model of kinematic diffraction is a new tool which can give accurate information about strain and damage in imperfect crystalline films[2]. It may therefore yield information about structural characteristics that may explain these differences. The present contract is for a study of implantation and annealing in GaAs and other materials by this technique, as well as by backscattering spectrometry (BSS).

We have conducted double crystal x-ray diffraction measurements on Si, Ge, and GaAs and shown that the strain induced by implantation is linear with implantation dose for Si and Ge, but non-linear in GaAs[1]. We have also shown that after implantation in GaAs to intermediate doses, for which the layer

is not amorphous, in addition to point defects, there appear certain extended defects[1]. These defects include long-range, gentle undulation of lattice planes and have a density on the order of $1/\mu m^2$. We have speculated that the non-linear strain versus dose and the creation of extended defects were caused by a transition from elastic to plastic distortion of the lattice. Such a transition is consistent with several experimental results. We therefore suggested that the poor, non-linear regrowth of GaAs at low temperatures can be attributed to such extended defects occurring initially at the interface between amorphous and crystalline regions. Since for thin films the yield strain increases inversely with the layer thickness and inversely with the strain gradient, we have proposed the use of multiple implants with varying species, energies and doses as a way of preventing the transition from elastic to plastic behavior. We have tested this approach and found that it did not result in improved low-temperature regrowth. In Section 3, we give details of our attempt.

We have also attempted to determine the basic source of the strain in GaAs, i.e., is it related to the presence of implanted ions or to the damage they create during nuclear stopping? Our results indicate that in the region where the strain is linear with dose, the strain is attributable to damage, i.e. point defects.

2. Experiments and Analysis

(100) GaAs samples were cleaned and etched lightly before implantation. During implantation, they were misoriented by 7° from normal to the ion beam to prevent channeling of the ions. Selected samples were annealed in flowing forming gas at 418°C for 60 min. All the samples were analyzed by x-ray diffraction and some were analyzed by backscattering spectrometry.

X-ray diffraction was conducted in air with a two-crystal diffractometer. X-rays from a tube with an Fe target are collimated and diffracted by a first crystal of virgin GaAs which has been adjusted to the same Bragg angle as that chosen for the sample. This serves to reduce the beam divergence and select the characteristic Kα line. The beam is then allowed to impinge on the sample, and x-rays diffracted from it are sensed with a NaI(Tl) detector. The sample is oriented close to the Fe Kα (400) Bragg angle and rotated finely through typically less than 1° and the reflecting power recorded as a function of angle to give the so-called "rocking curve". The experimental rocking curve is fitted with a calculated curve obtained with a kinematical diffraction model from a trial distribution of strain and damage[2].

Backscattering was conducted in an evacuated target chamber with 1.5 MeV He^+ ions from a van de Graaff accelerator. The ions are collimated and allowed to impinge close to normal to the

sample. Backscattered ions are detected by a Si surface barrier detector mounted at a scattering angle of 170°. Signals from the detector are sorted according to height to give backscattering spectra. The sample is rotated finely about two axes until the beam is incident on the (100) axis for "channeled" spectra or misoriented by 7° from the axis and rotated continuously about the beam axis for "random spectra".

3. Results and Discussion

3.1 Evolution of Strain and Damage Profiles with Implantation Dose.

In Fig. 1, we reproduce a figure from a previous report showing strain (solid lines) and damage, U (dashed lines) distributions obtained with 300 keV Si^+ implantations in GaAs. From Fig. 1(a) to (b), the dose changes from 2 x $10^{13}/cm^2$ to 1.5 x $10^{14}/cm^2$, but the maximum strain increases by only 20%. In this dose range, the strain at all depths saturates strongly, resulting in the broad profile of Fig. 1(b). The saturation value (0.45%) is close to the reported yield strain of externally stressed <110> GaAs[3]. As the implantation dose increases to 3 x $10^{14}/cm^2$, Fig. 1(c), there is a sharp rise in the strain of the central region. For doses above 3 x $10^{14}/cm^2$, the lateral coherence (uniformity) of the layer deteriorates. At a given depth, there are variations of ~ 0.01% in the strain and/or variations of ~ 2 arcmin in orientation. At 1.2 x $10^{15}/cm^2$, Fig.

1(d), the outer portion of the implanted layer has been rendered amorphus, but a damaged crystalline region remains at the interface with the substrate. This region contains the lateral variations mentioned above.

Figure 2 shows the BS spectra for the samples of parts b-d of Fig. 1. For doses of 1.5 and 3.0 x 10^{14} ions/cm^2, damage and strain in the lattice is evidenced only by increased dechanneling. At 1.2 x 10^{15} ions/cm^2, the channeling yield from the implanted region reaches that for randomly-aligned material, confirming that it has become amorphous to a depth of 3000 Å.

As we have reported previously, R.T. implantation with 300 keV Ne^+ or 300 keV P^+ results in similar behavior of the strain as a function of dose. Implantation with 300 keV P^+ at LN_2 temperature results in a more rapid increase of strain and damage with dose, but does not change the basic features seen with room temperature implantation.

3.2 Comparison of Strain with Nuclear Energy Deposition.

The non-linear behavior of the strain with dose may be attributed to self-annealing during implantation or to a transition from elastic to plastic deformation. The linear rise seen at low doses suggests that in this region the strain is simply related to parameters which increase linearly with dose, such as nuclear energy deposition density (F_D) or the local

concentration of stopped ions. In Fig. 3, we have compared the strain profile obtained with 300 keV Si^+, 2 x $10^{13}/cm^2$ with calculated F_D and Si concentration distributions[4]. The agreement between the shapes of the strain and F_D curves suggests that the source of the strain is the energy deposited in nuclear stopping.

Assuming a linear relation between the number of point defects and energy deposited by the ions in nuclear processes, it follows that the damage parameter U should vary linearly with strain at low doses. However, at low damage levels the sensitivity of the rocking curve to damage is much lower than that to strain. We can only say that at low doses the rocking curves are consistent with a linear relation between U and strain. For high doses, a non-linear relation seems to be required, as will be shown later.

Another way of testing the hypothesis that at low doses the strain is linear with F_D is to compare doses for different ion species resulting in the same (below-saturation) strain. We have determined experimentally the doses corresponding to 0.1% peak strain for implantation with Te^{++}, P^+, Si^+, Ne^+ and H^+. If the relation between strain and F_D is unique, there should be an inverse relationship between dose and F_D for various implanted species. Figure 4 shows that this is the case with the species tested. We shall further test this relation for implantation with B^+ and several other species.

3.3 Attempt to Improve Low-Temperature Regrowth of GaAs.

One objective of this project was to test whether the low-temperature regrowth of amorphized GaAs layers can be improved by the use of multiple energy and dose pre-implantation. In lattice mis-matched epitaxially-grown films, it has been shown that misfit dislocations may be avoided by incorporation of a graded strain profile[5]. In GaAs (and several other crystals studied), implantation produces an expansion of the unit cell, thus creating a lattice mismatch between the implanted layer and underlying undamaged material. For typical single energy implantation at doses sufficient to amorphize the layer, the transition between regions of high strain and nearly zero strain occurs over several hundred Å. We have suggested that if this region can, by multiple implantation, be made several thousand Å thick, thus reducing the strain gradient by an order of magnitude, the transition to plastic behavior might be avoided[6], and low-temperature regrowth would be better. We tested this hypothesis and found a negative result.

We chose Te as the doping ion because it is often used in practical applications. An energy of 500 keV was selected to produce a layer thickness of about 2000 Å. For this and greater layer thicknesses, the rocking curve is very sensitive to lateral non-uniformities, as might be created by extended defects. Figure 5(a) shows the measured and calculated rocking curves and strain and damage profiles obtained with a dose of 5×10^{12}

ions/cm^2. The peak strain is 0.48%, indicating that we are already in the saturation region. For this dose, there is no evidence of lateral non-uniformity. Figure 5(b) shows rocking curves and strain and damage profiles obtained for a dose of 1×10^{14} ions/cm^2. The backscattering spectrum indicates that the GaAs layer has been rendered amorphous to a depth of 2200 Å. The rocking curve is insensitive to the presence of an amorphous layer on top of crystalline material. The reflecting power of the amorphous layer is nearly zero and corresponds to U $\sim$ 0.4 Å.

The rocking curve does indicate the presence of a layer 500 Å thick in which the strain varies from 0.5% to zero, but gives no information about its location. Therefore it was drawn at what was considered to be its most likely location - directly beneath the amorphous layer. We will shortly compare the thermal regrowth of this layer to that of a region incorporating a graded strain layer obtained with triple Ne^+ implantation.

Figure 6 shows rocking curves, and strain and damage profiles, obtained with Ne^+ implantations at (a) zero dose, (b) 300 keV, 2×10^{13} ions/cm^2, (c) 140 keV, 1×10^{14} ions/cm2, and (d) 60 keV, 1×10^{14} ions/cm^2. If the strain behaved linearly with dose, the combination of these three implants would produce a graded strain profile beneath a 2000 Å amorphous layer. However, combination of the two higher energy implants with twice the dose of the low energy implant did not result in an amorphous surface layer. Figure 7(a) shows rocking curves, strain and

damage profiles and BS spectrum for the triple Ne^+ implant. The surface strain is 0.45%, i.e., the saturation value seen for intermediate doses, independent of ion species. Several doses of 500 keV Te^{++} ions were implanted after triple Ne^+ implants. Figure 7(b) shows that the introduction of 1×10^{12} Te ions/cm^2 resulted in a strain spike located 500 Å below the surface. The sharp strain peak in this region is similar to what is observed earlier for single energy Si^+, Ne^+ and P^+ implantations at high doses. We are unable to explain its shape. Another intriguing feature is an apparent rise in the damage at depths greater than the expected range of Te ions (compare the U -distributions in Figs. 7(a) and (b)). The strong oscillations in the rocking curves of Figs. 7(a) and (b) indicate that lateral coherence is maintained. For a Te dose of 1×10^{13} ions/cm^2 (Fig. 7(c)) the surface region remains crystalline, but has become laterally non-uniform, as shown by the suppression of oscillations. Thus even at this stage, where the Te dose has not rendered the surface layer amorphous, we observe the occurrence of extended defects seen earlier with single-energy implantations. The graded strain profile, prepared with the multiple Ne implantations failed to prevent them from forming. In Fig. 7(d), the Te dose of 1×10^{14} ions/cm^2 has amorphized the surface layer. The transition region between amorphous and strained crystalline regions is laterally non-uniform.

Figure 8 shows the results of annealing for 1 hr in

forming gas at 418°C. The sample implanted only with Te to 5×10^{12} ions/cm^2 (Fig. 8(a)) has regrown leaving a 2000 Å thick region with a strain of about 0.03%. As shown by the channeling spectrum in Fig. 8(b), the sample implanted to 1×10^{14} ions/cm^2 remains highly damaged. The triple Ne^+ implant did regrow almost completely, as seen in Fig. 8(c). However, the sample with the multiple Ne^+ implants plus Te^{++} to 1×10^{14} ions/cm^2 (Fig. 8(d)) remains very highly damaged in the region penetrated by the Te.

Thus our attempt to improve the low temperature regrowth of amorphized GaAs was a failure. It is not clear whether this is because our hypothesis about the role of extended defects in disrupting low-temperature regrowth is incorrect, or because we simply failed to prevent them from occurring. Several other questions remain. We do not understand the sharp strain spike which occurs at high doses with every species we have studied. Also, we do not understand the details of how, following the strain spike, the crystal breaks into incoherent domains.

4. Instrumentation and Software Development.

The two crystal x-ray diffractometer was developed for this project. It incorporates a microprocessor-controlled step scan apparatus for rocking the sample in steps of 0.0001 degrees.

Software was written for transferring data from the

microprocessor to a host computer, and existing programs adapted for video display. An existing program for fitting rocking curves with a kinematical diffraction model was adapted for the present application. General plotter graphics routines were written for producing plots of rocking curves, strain and damage profiles, BS spectra, etc.

Delivery of a replacement beam line extension for the back-scattering system is scheduled for September 1983.

5. Summary

5.1 Objective.

The objective of this project is to study the effects of ion implantation and thermal regrowth on the strain and damage in GaAs and other semiconductor materials by x-ray diffraction and backscattering spectrometry. The motivation for this study, and the potential of x-ray diffraction for yielding useful information about these materials are outlined in Section 1.

5.2 Technical Problem.

Unlike the case for Si and Ge, amorphized layers in GaAs do not regrow linearly with time during annealing, they regrow poorly at low temperatures, and only have significant electrical activation after annealing at relatively high

temperatures. The reasons for these differences are presently not known.

5.3 Method.

Experiments consist of implantation of GaAs with various ions at several doses and energies, at room temperature and LN_2 temperature, annealing at 418°C in flowing forming gas, and analysis by two crystal x-ray diffraction and channeled backscattering spectrometry. See Section 2 for details. Backscattering spectra were analyzed by standard techniques, which gave the thicknesses of amorphous layers, and qualitative information about damage densities. X-ray rocking curves were fitted by means of calculations of diffraction, based on a kinematic model. These yield profiles of strain and damage in the samples, as well as information about the lateral uniformity of the strained layers.

5.4 Results.

5.4.1 Evolution of Strain and Damage Profiles with Implantation dose.

At very low doses, the distribution of implantation-induced strain in GaAs appears to follow the profile of energy deposited in nuclear interactions. As the implantation dose increases, the strain in a narrow region (several hundred Å)

within the region that was formally saturating, rises very rapidly with dose, while the remainder of the profile evolves as before. At high doses, as the most highly strained region approaches amorphicity, the still-crystalline strained layers become laterally non-uniform with variations in the strain at a given depth of ~ 0.01% and/or variations of ~ 2 arcmin in orientation. We speculated that this is the result of plastic deformation of the lattice. This general behavior seems to be independent of ion species or energy, and occurs for implantations at both room and LN_2 temperature. See Sections 3.1 and 3.2.

5.4.2 Comparison of Strain With Nuclear Energy Deposition.

The reciprocal of the dose required to reach a constant below-saturation strain appears to scale linearly with the density of nuclear energy deposition. See Section 3.2.

5.4.3 Attempt to Improve Low-Temperature Regrowth of GaAs.

An attempt was made to improve the regrowth of amorphized Te-implanted GaAs layers by reducing the strain gradient beneath this layer by a factor of 10 with a multiple-energy implantation of Ne ions. The hope was that a reduced strain gradient would eliminate the transition to plastic

deformation. The attempt was unsuccessful: the lateral non-uniformities (attributed to plastic deformation) appeared as before, and thermal regrowth at 418°C was no better than for a sample that had been implanted with Te alone. See Section 3.3.

5.5 Important Conclusions.

Our conclusions at this stage are the following:

- At low implantation doses, the strain in GaAs appears to be determined by the energy deposited in nuclear interactions.

- Lateral non-uniformities occur at high implantation doses.

- Reducing the gradient of the strain by pre-implantation does not prevent the formation of these non-uniformities.

5.6 Hardware Development.

A two crystal x-ray diffractometer was built. See Section 4.

5.7 Comments and Implications for Further Research.

We were unable to prevent the lateral non-uniformities from occurring and then to compare thermal regrowth with that obtained when they are present. Consequently, the hypothesis that the lateral non-uniformities disrupt low-temperature regrowth remains untested. Also, many of our observations remain unexplained. For example, the origin of the sharp strain peak and the mechanism of the loss of lateral uniformity are not understood.

References

1. V. S. Speriosu, B. M. Paine, M-A. Nicolet, and H. L. Glass, J. Appl. Phys. 40 (1982) 604.

2. V. S. Speriosu, J. Appl. Phys. 52 (1981) 6094.

3. H. Booyens, J. S. Vermask, and G. R. Proto, J. Appl. Phys. 49 (1978) 5435.

4. K. B. Winterbon, Ion Implantation Range and Energy Distributions, (Plenum, New York, 1975), Vol. 12.

5. G. A. Rozgonyi, P. M. Petroff, and M. B. Panish, Appl. Phys. Lett. 24 (1974) 251.

6. C. A. Ball and C. Laird, Thin Solid Films, 41 (1977) 307.

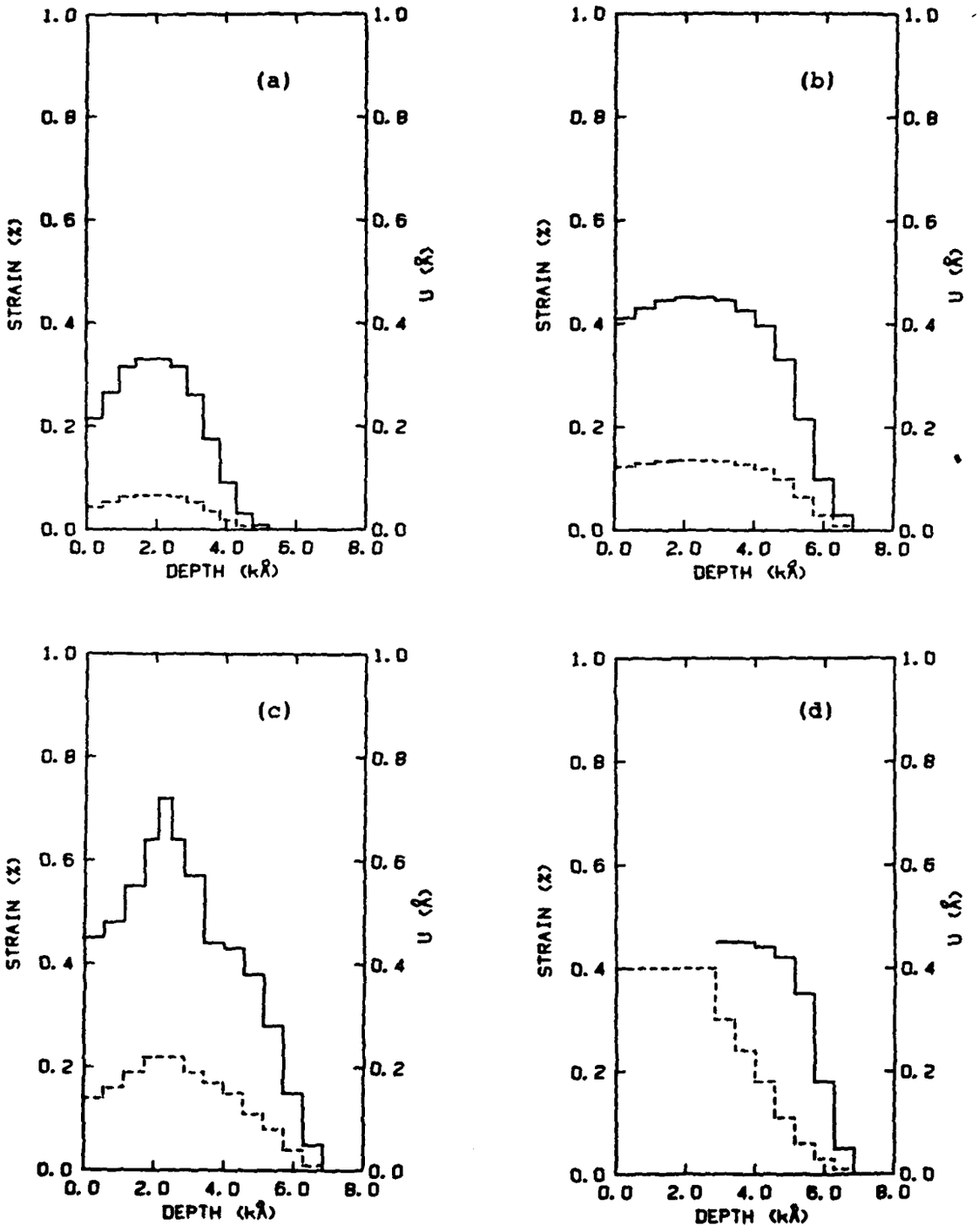

Fig. 1. Strain (solid lines) and damage (dashed lines) profiles for R.T. 300 keV Si^+ implantation. Doses are (a) 2×10^{13}, (b) 1.5×10^{14}, (c) 3.0×10^{14}, (d) 1.2×10^{15} ions/cm^2.

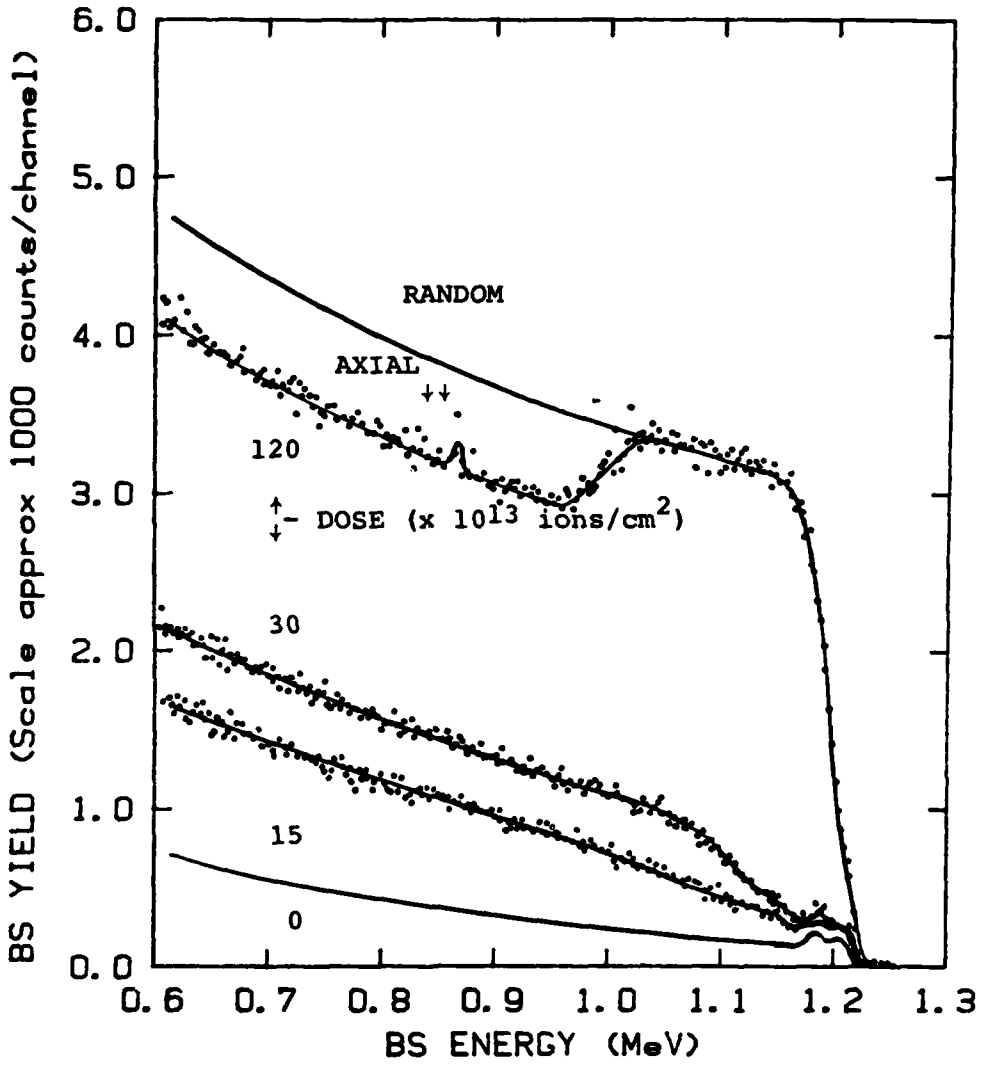

Fig. 2. Channeling spectra for the samples of Fig. 1 parts b, c, and d. Spectra for random orientation, and axially-aligned orientation of an unimplanted sample are also shown.

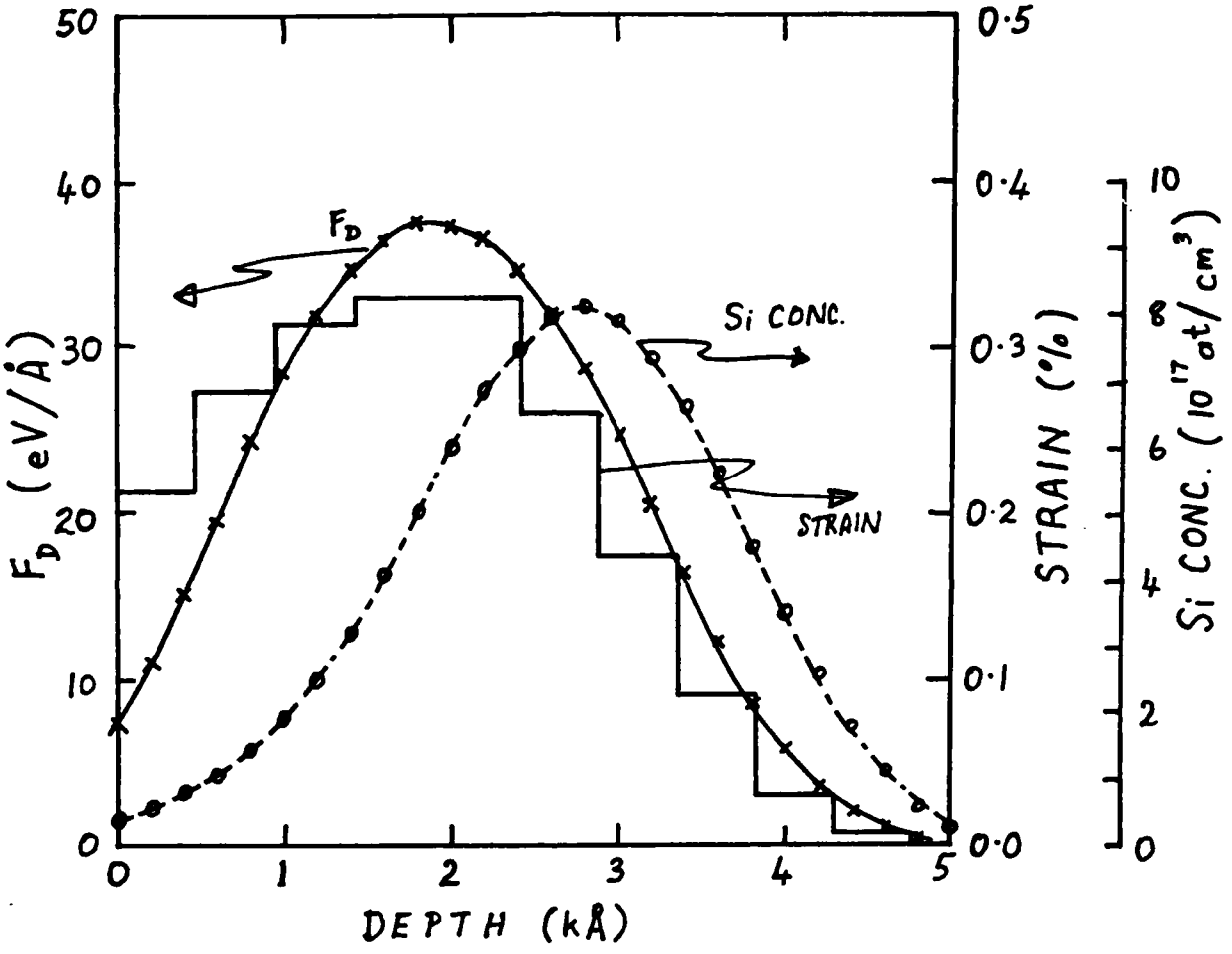

Fig. 3. Comparison of profiles of strain, nuclear energy deposition density (F_D) and Si concentration for implantation of 300 keV Si^+ to 2 x 10^{13} ions/cm^2.

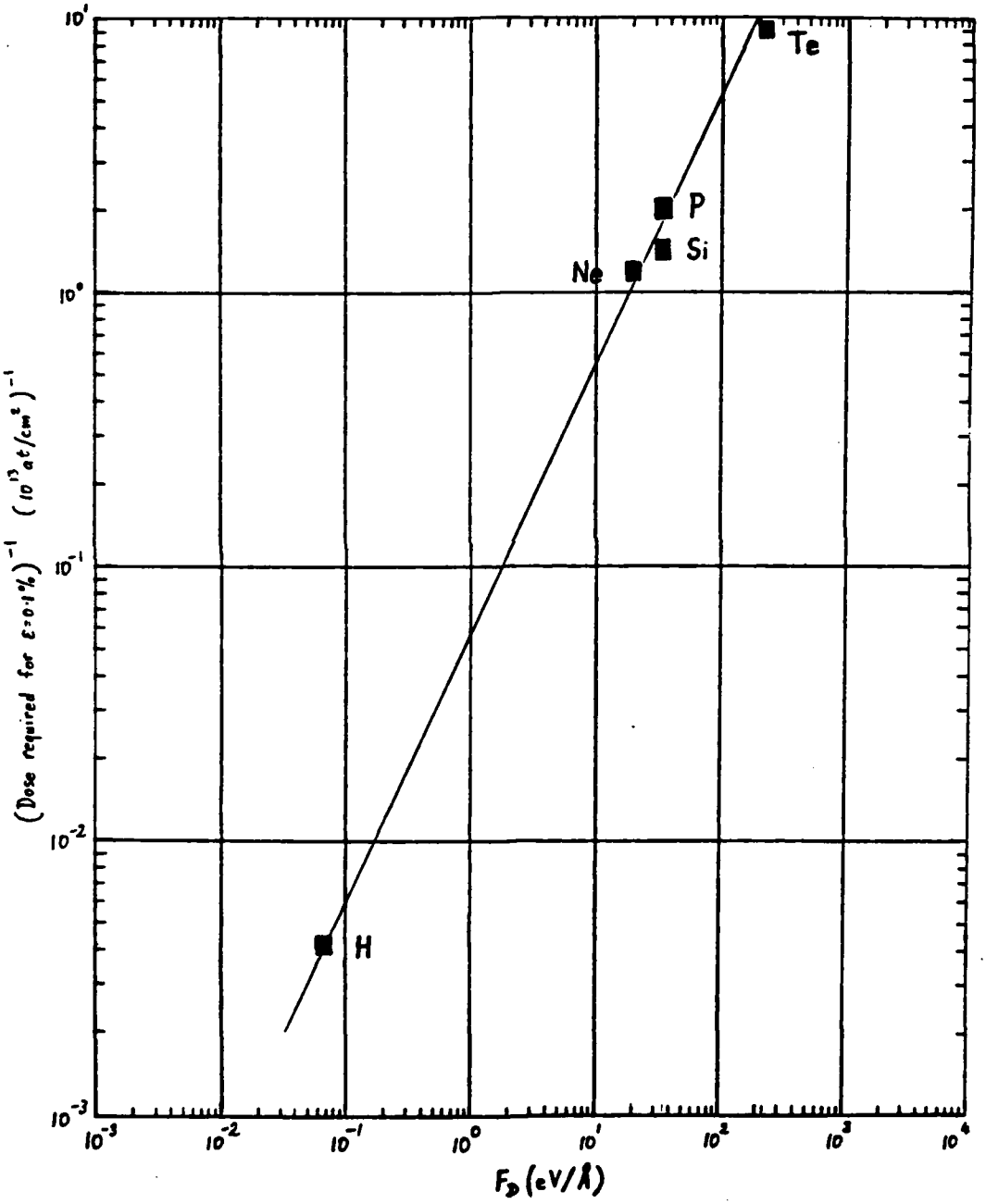

Fig. 4. Reciprocal of dose versus nuclear energy deposition density for implantation of 5 species in GaAs.

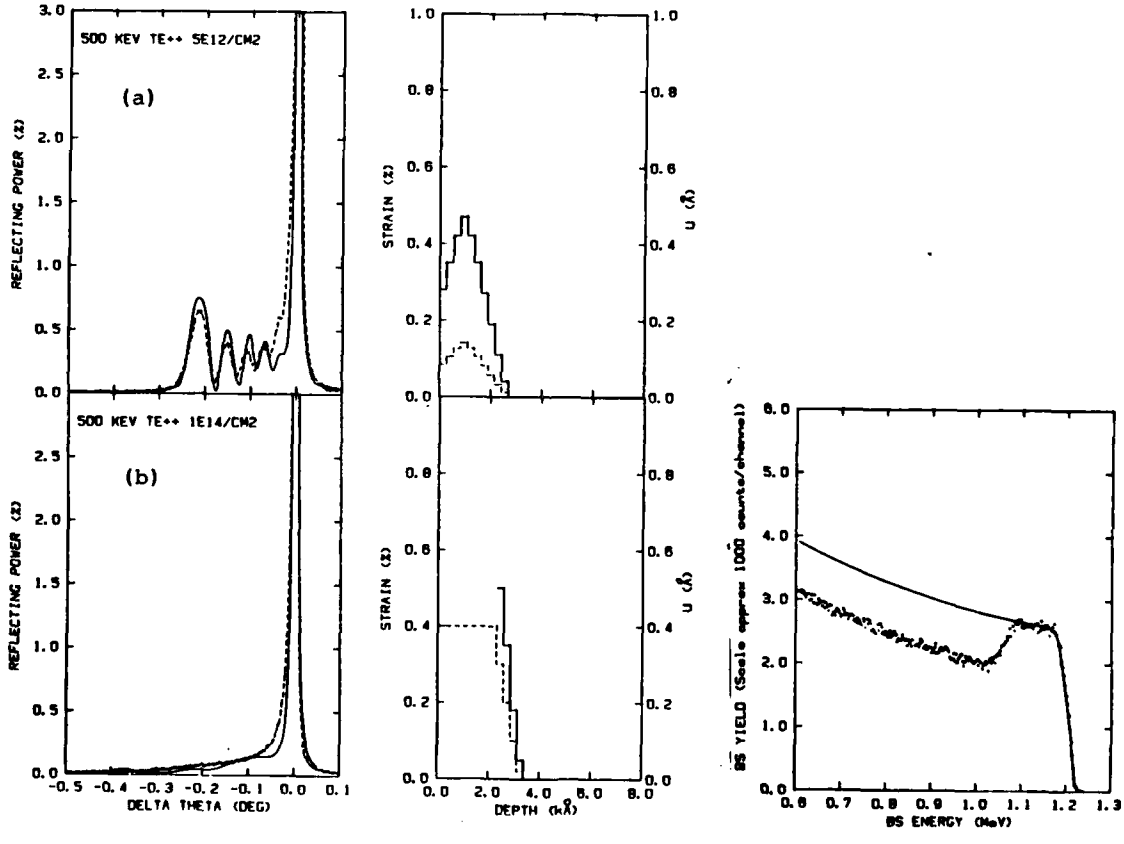

Fig. 5. Rocking curves and strain and damage profiles for two doses of Te++ implantation. Also shown for case (b) is the channeled BS spectrum (data points) and the random spectrum (solid lines).

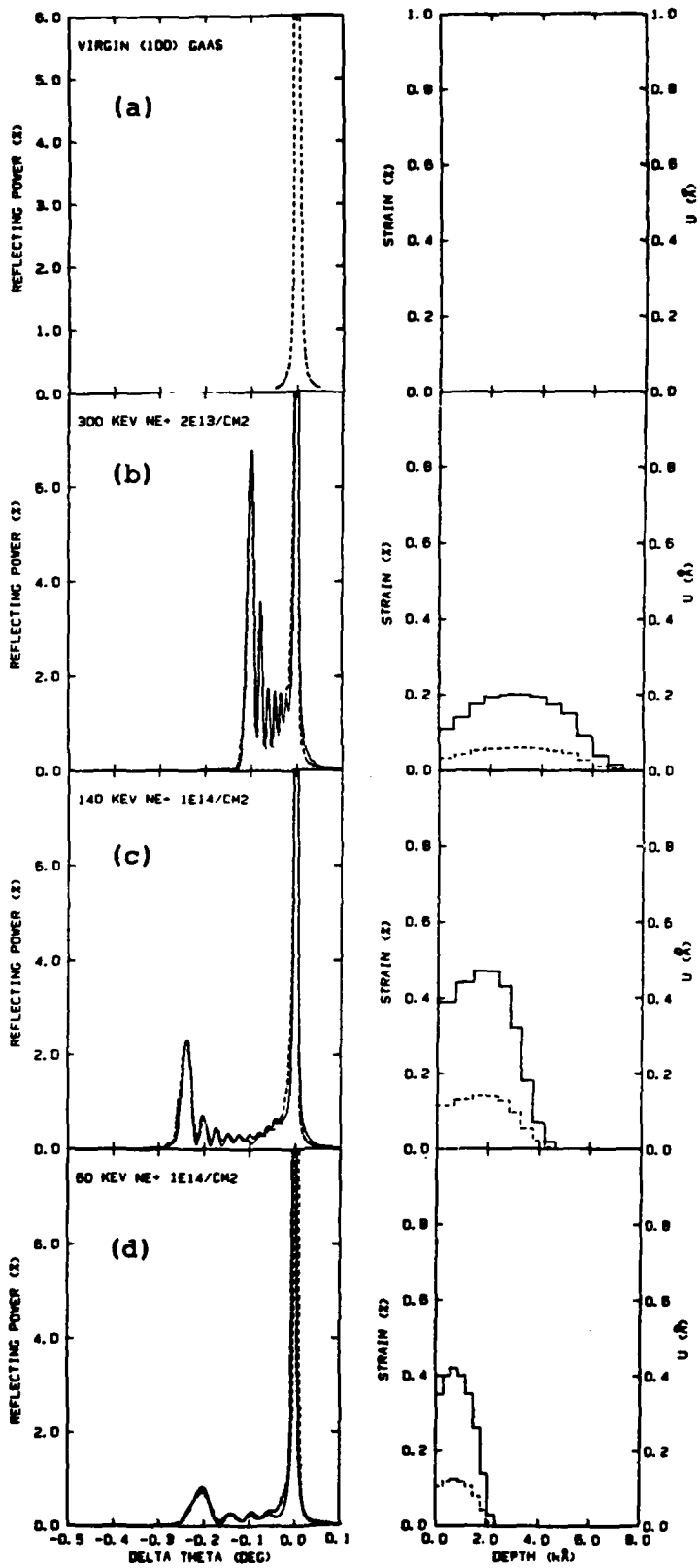

Fig. 6.

Left-side: measured (dashed) and calculated (solid) rocking curves for virgin and Ne^+-implanted GaAs with three different ion energies and doses.

Right-side: corresponding strain and damage profiles.

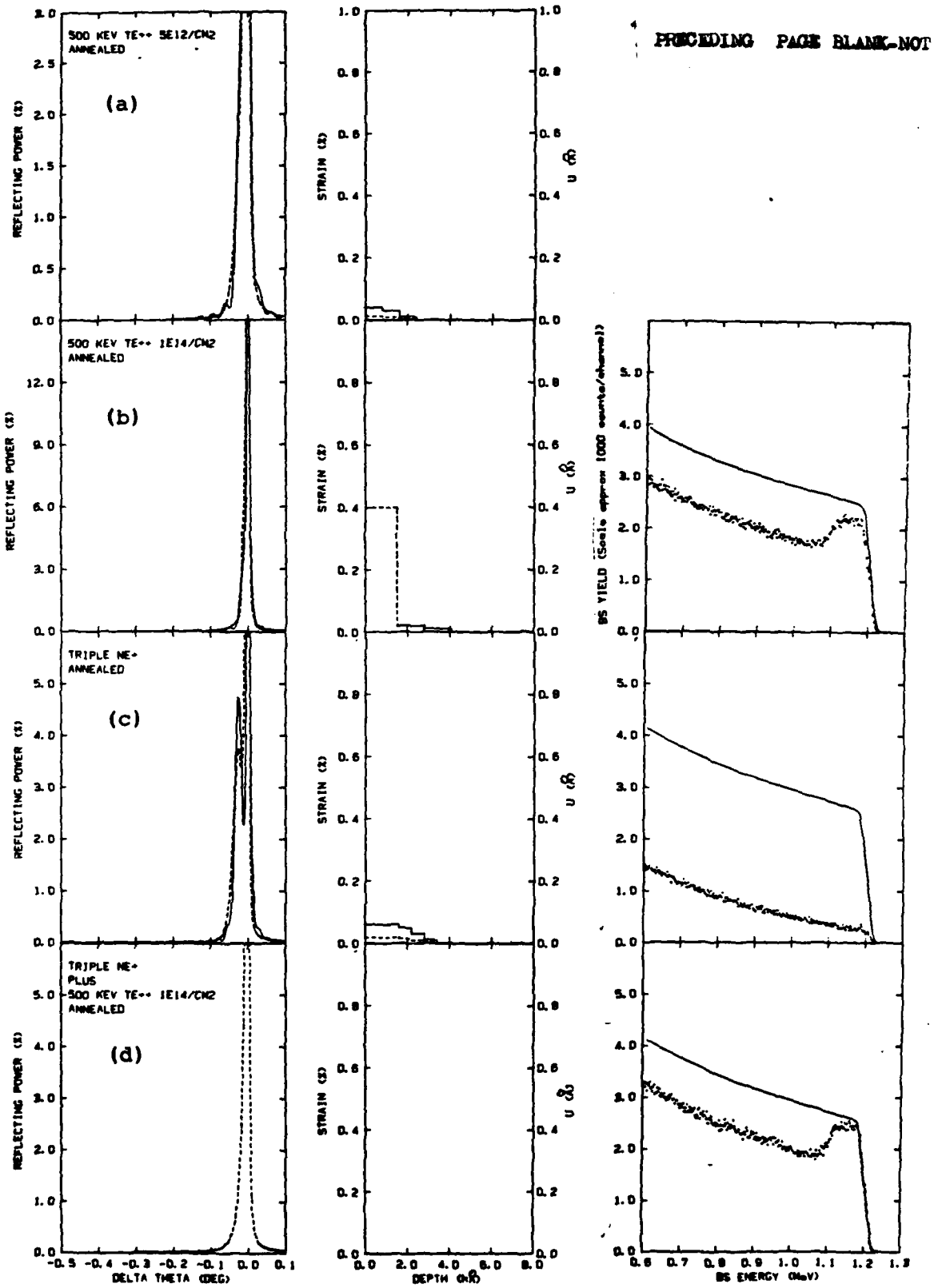

Fig. 8. Rocking curves, strain and damage profiles and BS spectra for annealed samples.